Geofísica Internacional (2024) **63-4**: 1225 - 1238

Characterization of $PM_{2.5}$ during the ACU15 campaign in Mexico City

Telma Castro[1], Oscar Peralta[1], Cristina Prieto[3], Naxieli Santiago[1], Harry Alvarez-Ospina[2], Rocío García[1], Isabel Saavedra[1], María de la Luz Espinosa[1], Enrique Hernández[3], Javier Miranda[4], Violeta Gómez[3], Corina Solís[4], Dara Salcedo[5], Ricardo Torres-Jardón[1], Amparo Martínez-Arroyo[1], Abraham Ortínez-Alvarez[3], Gerardo Ruíz-Suárez[1] and Elba Ortiz[6]

Abstract

We collected daily $PM_{2.5}$ samples from January 19 to March 20, 2015, in the south of Mexico City and performed chemical analysis. The analyses showed an overall composition of 39% organic carbon, 12% elemental carbon, 20% water-soluble ions (NO_3^-, SO_4^{-2}, Cl^-, Na^+, K^+, NH_4^+, and Ca^{2+}), and 23% elements (Al, Si, S, P, Cl, Cr, Mn, Fe, Pb, and Hg) in mass. Sulfur and phosphorus showed a correlation coefficient 0.91, likely indicating fossil fuel emissions. The samples contain secondary inorganic aerosols typical of urban areas, and the oxidation ratios of sulfur and nitrogen suggest that oxidative reactions from vehicle emissions probably produce them. Furthermore, modern carbon in $PM_{2.5}$ represents half of the total carbon, indicating carbon sources other than fossils.

Key words: Mexico City Metropolitan Area, $PM_{2.5}$, radiocarbon, secondary inorganic aerosols.

Resumen

Recolectamos muestras diarias de $PM_{2.5}$ del 19 de enero al 20 de marzo de 2015 en el sur de la Ciudad de México y realizamos análisis químicos. Los resultados de los análisis mostraron una composición general de 39% de carbono orgánico, 12% de carbono elemental, 20% de iones solubles en agua (NO_3^-, SO_4^{-2}, Cl^-, Na^+, K^+, NH_4^+, and Ca^{2+}) y 23% de elementos (Al, Si, S, P, Cl, Cr, Mn, Fe, Pb y Hg) en masa. El azufre y el fósforo mostraron un coeficiente de correlación de 0.91, lo que probablemente indica emisiones de combustibles fósiles. Las muestras contienen aerosoles inorgánicos secundarios típicos de las zonas urbanas y los cocientes de oxidación del azufre y el nitrógeno sugieren que probablemente las reacciones oxidativas de las emisiones de los vehículos los produzcan. Además, el carbono moderno en $PM_{2.5}$ representa la mitad del carbono total, lo que indica fuentes de carbono distintas de los fósiles.

Palabras clave: Área Metropolitana de la Ciudad de México, $PM_{2.5}$, radiocarbono, aerosol inorgánico secundario.

Received: Octubre 6, 2023; Accepted: July 3, 2024; Published on-line: October 1, 2024.

Editorial responsibility: Dra. Ofelia Morton-Vermea

* Corresponding author: Corresponding author: Oscar Peralta, oscar@atmosfera.unam.mx

[1] Instituto de Ciencias de la Atmósfera y Cambio Climático, Universidad Nacional Autónoma de México, Ciudad Universitaria, 04510 Coyoacán, CDMX, México.

[2] Facultad de Ciencias, Universidad Nacional Autónoma de México, Ciudad Universitaria, 04510 Coyoacán, CDMX, México.

[3] Posgrado en Ciencias de la Tierra, Universidad Nacional Autónoma de México, Ciudad Universitaria, 04510 Coyoacán, CDMX, México.

[4] Instituto de Física, Universidad Nacional Autónoma de México, Ciudad Universitaria, 04510 Coyoacán, CDMX, México.

[5] UMDI-Juriquilla Facultad de Ciencias, Universidad Nacional Autónoma de México, Blvd. Juriquilla 3001, 76230 Querétaro, México.

[6] Universidad Autónoma Metropolitana-Azcapotzalco, Av. San Pablo 180, 02200 CDMX, México.

Telma Castro, Oscar Peralta, Cristina Prieto, Naxieli Santiago, Harry Álvarez-Ospina, Rocío García, Isabel Saavedra, María de la Luz Espinosa, Enrique Hernández, Javier Miranda, Violeta Gómez, Corina Solís, Dara Salcedo, Ricardo Torres-Jardón, Amparo Martínez-Arroyo, Abraham Ortínez-Alvarez, Gerardo Ruíz-Suárez, Elba Ortiz.

https://doi.org/10.22201/igeof.2954436xe.2024.63.4.1745

1. Introduction

The Mexico City Metropolitan Area (MCMA) covers 7,866 km^2, comprising 16 municipalities of Mexico City, 59 municipalities of the State of Mexico, and one municipality of Hidalgo. It is a region with a long history of poor air quality, where more than 22 million people live and daily make 15.6 million trips on public transportation (three out of every four are used by bus, and the Metro occupies the second place in frequency of use, with 29% of trips) and 6.6 million car trips, with an average of 1.5 occupants per vehicle (Geografía, 2017)

Since 2010, Mexico City authorities have published emissions inventories for criteria pollutants. The particle matter with 2.5 μm aerodynamic diameter ($PM_{2.5}$) emission in 2014 was more than 12 gigagrams (Gg); in 2016 dropped to 5 Gg, and in 2018 increased to more than 16 Gg. That year, the mobile sources emitted more than 7 Gg of $PM_{2.5}$, 698 Gg of CO, 124 Gg of NOx, and 1 Gg of SO_2. So, transportation is the sector that contributes the most pollutants to the environment (México, 2021). Also, thirty thousand industries continually release tens of metric tons of particulate matter and polluting gases into the atmosphere every year. Although some pollutant concentrations have decreased, $PM_{2.5}$ has remained almost the same since 2010. For example, in 2018, only one peri-urban monitoring station was below the national $PM_{2.5}$ standard. Thus, chronic exposure to $PM_{2.5}$ is associated with threatening inhabitants' health, and heavy-duty vehicles in MCMA produce around 10% of $PM_{2.5}$ (Evans *et al.*, 2021).

Many secondary inorganic aerosols (SIA) result from gases and aqueous phase oxidation reactions of primary and secondary pollutants. Ammonium, nitrates, and sulfates are the most relevant components of SIA. These compounds are hygroscopic, grow by condensation of water vapor and are common in polluted urban atmospheres such as the MCMA (Dat *et al.*, 2024; Squizzato *et al.*, 2013; Warneke *et al.*, 2013). SIA form ammonium sulfate ($(NH_4)_2SO_4$), ammonium nitrate (NH_4NO_3), and other nitrate salts (Chu *et al.*, 2023) impacting the air quality of the MCMA and regions nearby (Garzón *et al.*, 2015; Zavala *et al.*, 2020).

Sulfates can adversely affect human health and the environment. Nitrates also have health implications, particularly for respiratory conditions. The impact of particles on health in polluted urban atmospheres is well known, and the combination of physical and chemical properties of particulate matter (PM) also implies diseases associated with numerous health disorders (Bozkurt *et al.*, 2014; Davidson *et al.*, 2007; Echeverría *et al.*, 2023; Mamkhezri *et al.*, 2020).

In 2015, we carried out the Aerosols Campaign at UNAM (ACU15) on the main campus of the Universidad Nacional Autónoma de México (National Autonomous University of Mexico, UNAM) to characterize the chemical composition of $PM_{2.5}$, compare results with previous studies, and determine if the general chemical composition of the atmospheric aerosol has changed. This manuscript focuses on SIA measured during ACU15.

2. Methodology

The ACU15 campaign was carried out on the UNAM campus of Mexico City (19°19'34.12", 99°10'33.86). Meteorological instrumentation and air samplers were installed on the roof of the Instituto de Ciencias de la Atmósfera y Cambio Climático (Institute of Atmospheric Sciences and Climate Change, ICACC) at about 15 m above the ground. Green areas towards the west and south surround the sampling site. A residential zone and the metro and bus stations (~500 m) are towards the north and east. Vehicles and public transport circulate daily, and heavy trucks pass after midnight (Abanto *et al.*, 2020). Figure 1 shows the location of the measuring site.

The campaign occurred during the cold-dry season from January 19 to March 19, 2015. At the measurement site, there was also an air quality monitoring station belonging to the Red Automática de Monitoreo Atmosférico (Automatic Atmospheric Monitoring Network, RAMA) and a meteorological station belonging to the Programa de Estaciones Meteorológicas del Bachillerato Universitario (Program of Meteorological Stations of the University Baccalaureate, PEMBU). Both stations offer information to the public at **http://www.aire.cdmx.gob.mx/default.php?opc=%27aKBh%27** and **https://www.ruoa.unam.mx/pembu/index.php?page=historical_facts**.

2.1 Meteorology

PEMBU provided data on wind speed and direction, temperature, solar radiation, pressure, and humidity. The Red Universitaria de Observatorios Atmosféricos (University Network of Atmospheric Observatories, RUOA) provided the greenhouse gas concentration data, and RAMA the air criteria pollutants concentrations.

HYSPLIT (Hybrid Single-Particle Lagrangian Integrated Trajectory) is a trajectory model that calculates simple trajectories of air parcels and simulates the transport and dispersion of particles in the atmosphere. We used it to calculate the backward trajectories of parcels and determine the possible origin of air masses impacting the site to establish source-receiver relationships. We used HYSPLIT to calculate the backward trajectories at 50 m above the ground level (AGL) with 0.5-degree global meteorological information (GDAS) and 24 hours backward.

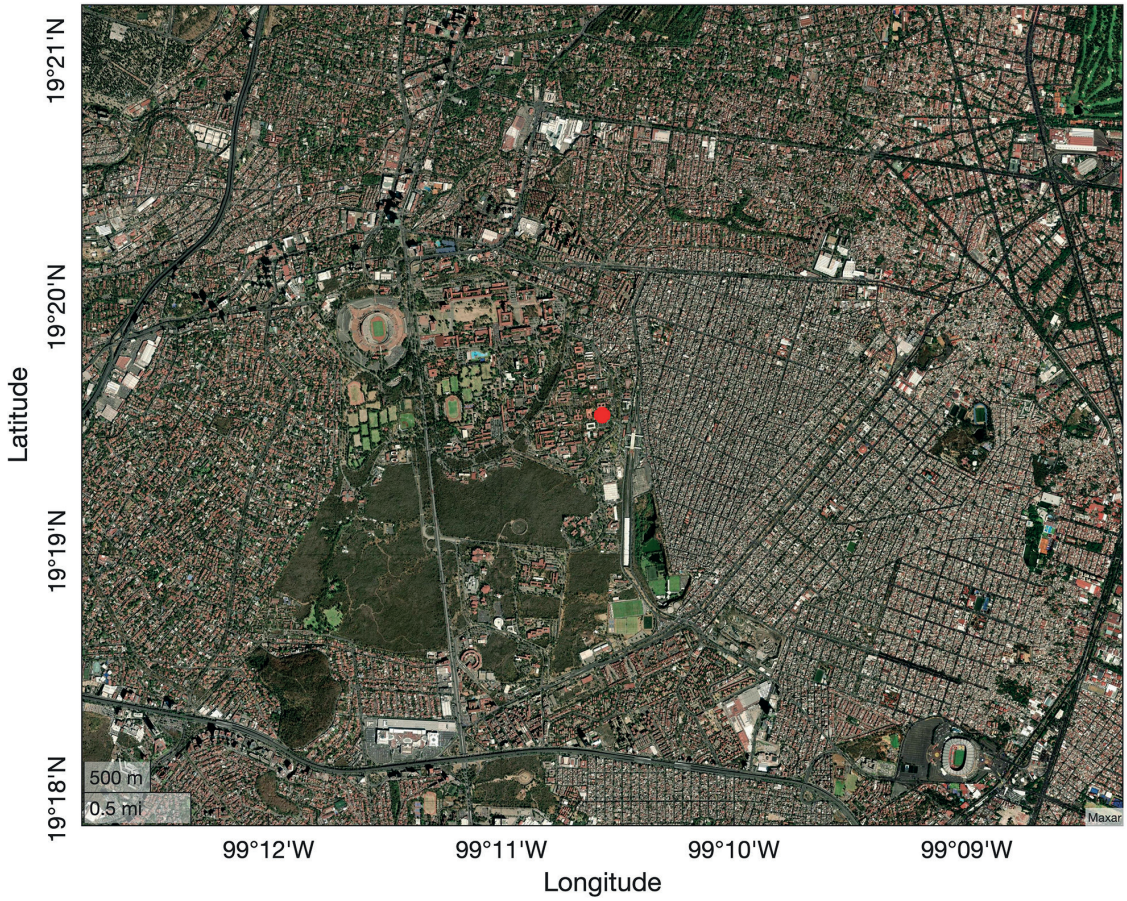

Figure 1. Location of the sampling site (red dot). The site was in the south of Mexico City.

2.2 Air quality

The RAMA routinely measures the concentration of criteria pollutants: NO, NO_2, CO, SO_2, O_3, PM_{10}, and $PM_{2.5}$, and reported one-hour average criteria pollutant concentrations. We downloaded the data from January 18 to March 31, 2015.

2.3 Particle sampling

We employed 47 mm Teflon and quartz filters to collect $PM_{2.5}$. Before sampling, Teflon filters were rinsed with deionized water and weighted on a semi-microbalance (Sartorious CPA225D). At the same time, quartz filters were preheated for six hours at 550 °C to eliminate all carbonaceous residues. They were conditioned for 24 h at 25 °C and constant relative humidity, and after that, weighed and stored individually in Petri dishes. After sampling, filters were placed in Petri dishes, wrapped with parafilm, and stored at 4 °C until the gravimetric analysis.

We collected 60 samples of $PM_{2.5}$ on quartz and 60 samples on Teflon substrates, both using MiniVol TAS (Airmetrics, USA) with a flow rate of 5 l min^{-1} ± 10%, on 24 hours sampling basis.

We also collected 30 samples on quartz substrates (Pallflex 2500 20 × 25 cm, QAT-UP; Pall Sciences, Ann Arbor, MI, USA) using a high-volume sampler (Graseby Andersen SA-2000H) operating at 1.9 m^3 min- for 48 hours. Samples were prepared and encapsulated in a tin crucible substrate for radiocarbon analysis.

2.4 Carbonaceous material

The carbon analyzer CM5014 (UIC, Inc) quantified the organic carbon (OC) and the total carbon (TC) of particle samples. The instrument measures the CO_2 gas stream produced from the complete combustion of carbonaceous material, which enters the coulombimetric cell and converts it into carbon content. The sample is heated at a fixed temperature. The OC evolved at 450 ºC and the TC at 700 °C (Alvarez-Ospina *et al.*, 2016). The difference between TC and OC corresponds to elemental carbon (EC), following the equation:

$$EC = TC - OC \quad (1)$$

2.5 Elements

$PM_{2.5}$ collected onto Teflon substrates was employed for different analytical techniques to determine the chemical composition of particulate matter. X-ray fluorescence (XRF) analyses were performed with a spectrometer based on Oxford Instruments, an X-ray tube with Rh anode, and an Amptek Si-PIN X-Ray detector (resolution 160 eV at 5.9 keV) (Díaz *et al.*, 2014; Reynoso-Cruces *et al.*, 2021). The detector efficiency was measured using a thin film standard set (MicroMatter, Vancouver, Canada). The X-ray tube operated at 50 kV and 500 µA, irradiating each sample for 900 s. The analyses provided results on Al, Si, Fe, P, S, Cl, Cr, Mn, and Pb concentrations. Uncertainties were evaluated as described by (Hernández-López *et al.*, 2020).

Mercury (Hg) was analyzed using an atomic absorption spectrophotometer coupled to the hydride vapor generator (AAS-HVG) (Model GBC 932, GBC Scientific Equipment, Inc., Hampshire, Illinois, USA). Supra-pure HCl and HNO_3 digested the Hg according to Method IO-5, using an SEM microwave oven for elemental composition analysis in an OES-ICP (Thermo-Jarrel).

2.6 Water-soluble inorganic ions

A Dionex ICS-1500 ion chromatographer (IC) measured anions (NO_3^-, SO_4^{-2}, and Cl^-) and cations (Na^+, K^+, NH_4^+, and Ca^{2+}). Anions analysis was performed using a Dionex IonPac AS23 column (4 × 250 mm) and cations with a Dionex IonPac CS12A column (4 × 250 mm). The mobile phase was a carbonate solution (Na_2CO_3 4.5 mM – $NaHCO_3$ 0.8 mM) for anions and methan- sulfonic acid (CH_4O_3S 20 mM) for cations at a flow rate of 1 ml min^{-1} for both ions. The limit of quantification (LOQ) and determination (LOD) were calculated using the linear regression of standards calibration. LOD and LOQ were calculated as follows and are shown in Table 1.

$$LOD = 3.3\left(\frac{\sigma}{s}\right) \tag{2}$$

$$LOQ = 3.3\ LOD \tag{3}$$

Where σ is the standard deviation of the response and s is the slope of the calibration curve.

Table 1. Detection (LOD) and quantification limits (LOD) of ion chromatographer, µg m^{-3}.

	Na^+	NH_4^+	K^+	Ca^{2+}	Cl^-	NO_3^-	SO_4^{2-}
LOD	0.01	0.09	0.01	0.01	0.03	0.07	0.09
LOQ	0.02	0.30	0.03	0.03	0.09	0.23	0.31

Also, an Aerosol Chemical Speciation Monitor (ACSM) measured the chemical composition of atmospheric aerosols in real time. It operates based on the principles of aerosol mass spectrometry, providing information on the concentrations of organic compounds and inorganic ions. Other authors have more information about the operation and calibration of ACSM during the measuring campaign (Prieto *et al.*, 2023; Salcedo *et al.*, 2018).

We calculated the sulfur (SOR) and nitrogen (NOR) oxidation ratios to identify the oxidation rate of the atmosphere by using equations 4 and 5 (chemical species concentrations are in mol m^{-3}):

$$SOR = \frac{SO_4^{2-}}{SO_4^{2-} + SO_2} \tag{4}$$

$$SOR = \frac{NO_3^-}{NO_3^- + NO_2} \tag{5}$$

SOR and NOR estimate secondary transformation processes from NO_2 to NO_3^- and SO_2 to SO_4^{2-}. Values above 0.1 suggest photo-oxidation in the atmosphere might have occurred (Zhang *et al.*, 2013).

The neutralization ratio (NR) in the atmosphere refers to the balance between the most abundant acidic and basic components, often expressed as the ratio of acidic to basic ions or compounds in the atmosphere. It is related to acid-base reactions involving aerosols and gases. A neutralization ratio higher than one indicates an excess of basic ions relative to acidic ions, suggesting a more neutral or alkaline atmosphere. Conversely, a ratio less than one indicates an excess of acidic ions relative to basic ions, suggesting a more acidic atmosphere. It can help to assess the effectiveness of pollution control measures and better predict future changes in atmospheric composition. The NR is in equivalent concentrations:

$$NR = \frac{NH_4^+}{NO_3^- + SO_4^{2-}} \tag{6}$$

2.7 Quality control and quality assurance

A tapered element oscillating microbalance (TEOM) was used as a reference for gravimetric analysis of $PM_{2.5}$. The instrument belongs to RAMA. The carbon analyzer was calibrated using the NIST SRM 1649a Urban Dust standard. For radiocarbon analysis by AMS, Oxalic acid II was used as a standard reference, and

blanks with no radiocarbon [phthalic acid ($C_8H_6O_4$)] were also measured to subtract the background (Solís *et al.*, 2017). The quality control and quality assurance (QC/QA) for Hg analyses were established using standard reference materials (SRMs), blanks, and blind samples in triplicate. The system calibration employed SRM NIST-2711 (Montana soil, certified Hg value 6250 ng g^{-1}), SARM-20 (Sasolburg bituminous coal, with Hg value of 250 ng g^{-1}), MESS-2 (Beaufort Sea estuarine sediment, certified Hg value 89 ng g^{-1}) and an internal laboratory standard (Hot Spring deposit, Hg value 330 ng g^{-1}). Accuracy verification for XRF was carried out using the NIST SRM 2783 (air particulate in filter media).

The curves with the standards were prepared with a multi-elemental standard (High Purity QC-TMFM-A) in 2% HNO_3 to QC/QA for elemental analyses, and duplicated analyses were carried out every five filters. SO_4^{-2} (chromatographic method) and S (XRF analysis) showed a good correlation (r = 0.90). All chemicals were analytical grade, and solutions were prepared using ultrapure water (18.2 MΩ).

2.8 Statistical analysis

We averaged the concentration data from instrument measurements over 24 hours to match particle sampling times. We also calculated the basic statistics and kurtosis of the ion chromatographer and the ACSM to compare the data results between both instruments. We used the Matlab 2020 program (Mathworks, Inc.) to perform the statistical calculations and create the figures.

3. Results

3.1 Meteorology

From January to March 2015, the predominant wind speed was below 1 m s^{-1}, blowing from west, south, and east. The temperature oscillated between 10 – 15 ºC, the relative humidity between 30 – 60%, and the rain was present only for two days. The atmospheric pressure oscillated between 773 and 780 mbar. All those meteorological measurements were common in the dry-cold season (winter) in the MCMA (Figure 2). The maxima daily solar radiation was above 600 W m^2, except on rainy days (February 14 and March 15).

During the rainy days, the temperature diminished, and the relative humidity increased without significant changes in the wind speed. Based on the HYSPLIT backward trajectories and the wind rose of Figure 2, weak air masses traveled from the south at 50 m AGL toward the sampling site. Figure 3 shows three consecutive days in January, three days in February, and three more days in March 2015, with similar trajectories.

3.2 Air quality

The average concentrations of O_3, NO_2, CO, and SO_2 were 27 ± 9 ppb, 23 ± 6 ppb, 0.79 ± 0.21 ppm, and 3.8 ± 3 ppb, respectively. NO_2, O_3, and SO_2 did not exceed the national standard air quality threshold, and CO was within the limit recommended by the World Health Organization (WHO). Figure 4 shows the

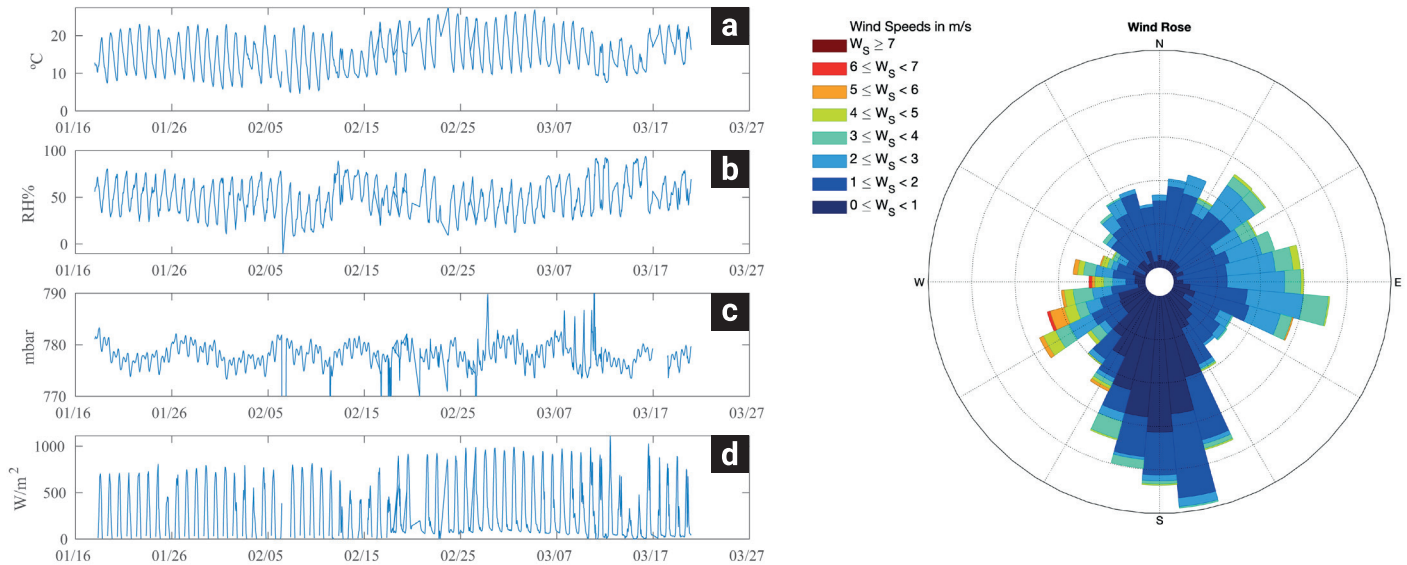

Figure 2. Meteorological parameters ACU15, Left: a) average temperature, b) relative humidity, c) atmospheric pressure, and d) solar radiation. Right: wind rose. Data source: PEMBU.

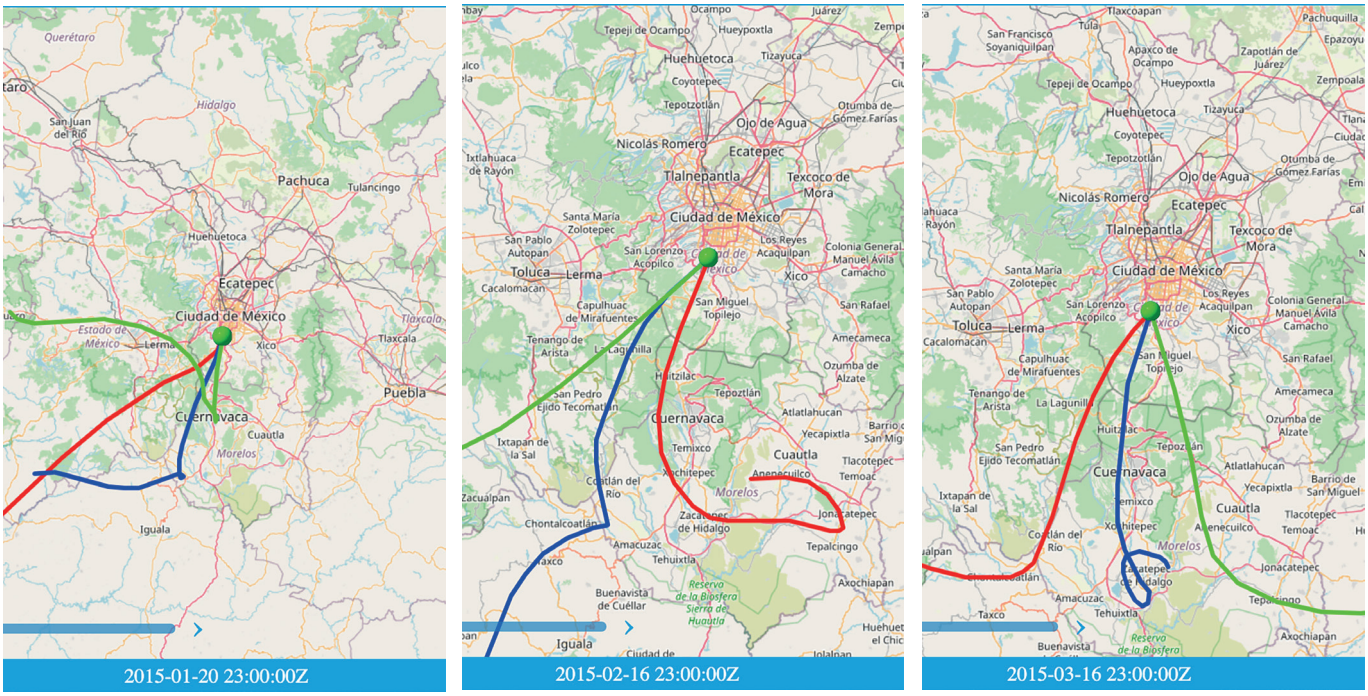

Figure 3. HYSPLIT backward trajectories January, February, and March 2015.

time series of daily average concentration for criteria pollutants. O_3, NO, and NO_2 decreased on February 3 and 14 and March 15. In fact, on March 15, all criteria gases were at minimum concentrations because the rain scavenged gases and particles from the atmosphere.

The bottom chart in Figure 4 shows the time series of $PM_{2.5}$ reported by RAMA and sampled with impactors in ACU15. They have a correlation coefficient of 0.73. January 20 was windy, and February 14 and March 15 showed different concentrations. Those were days with rain.

3.3 Particulate matter

The maximum concentration threshold for $PM_{2.5}$ is 25 $\mu g\,m^{-3}$ hourly average (NOM-025-SSA1-2020), and sometimes the $PM_{2.5}$ concentration was above that number. The Secretaría de Medio Ambiente de la Ciudad de México (Mexico City Environmental Secretary, SEDEMA) reported a $PM_{2.5}$ annual average concentration of 21.3 $\mu g\,m^{-3}$ and an average daily maximum concentration of 40 $\mu g\,m^{-3}$ in 2015 (INECC, 2016). So, the average concentration of $PM_{2.5}$ ($20.5 \pm 8.0\,\mu g\,m^{-3}$) at the measuring site was lower than the annual average of that report, and the $PM_{2.5}$ concentrations did not show any significant differences between weekdays and weekends.

3.4 Carbonaceous material and radiocarbon content

Organic carbon (OC) was the most abundant species in $PM_{2.5}$, with a concentration almost three times higher than EC, corresponding to 75% and EC to 25% of TC contents. The average concentration of OC was $8.06 \pm 1.85\,\mu g\,m^{-3}$, and for EC was $2.45 \pm 1.69\,\mu g\,m^{-3}$. The OC/EC ratio ranged from 1.40 to 9.56, with a mean of 3.74 ± 1.79 (Table 4). Based on the weak intensity of the wind, vehicles and other local activities near the site were likely the primary sources of carbonaceous material. Furthermore, the predominant wind came from the south, where there are no industries, so the transport of pollutants probably came from vehicles. However, the OC fraction had significant variations. So, both primary sources and secondary processes contributed to the OC concentration, resulting in a poor correlation coefficient between OC and EC ($r = 0.10$). EC corresponded to 12% and OC to 39% of the total particle mass, meaning carbonaceous material was around 51% of $PM_{2.5}$.

The OC represents primary (POC) and secondary organic carbon (SOC) (Chow *et al.*, 2002; Sharma *et al.*, 2018; Turpin & Huntzicker, 1995; Vega *et al.*, 2004). SOC concentrations reported by other authors during ACU15 campaign had a poor correlation with the main components of secondary inorganic aerosols (SIA) (Rosa *et al.*, 2024). Table 2 shows the results of the cross-correlation analysis.

The radiocarbon analysis provides a tool for measuring fossil versus no fossil sources. The fraction of modern carbon (pMC) in fossil fuel combustion is zero, while no fossil sources have a pMC close to 100%. The pMC in $PM_{2.5}$ varied from 41% to 59%, with an average of 50% ($n = 15$), indicating biomass burning and other processes than fossil fuel combustion originated half

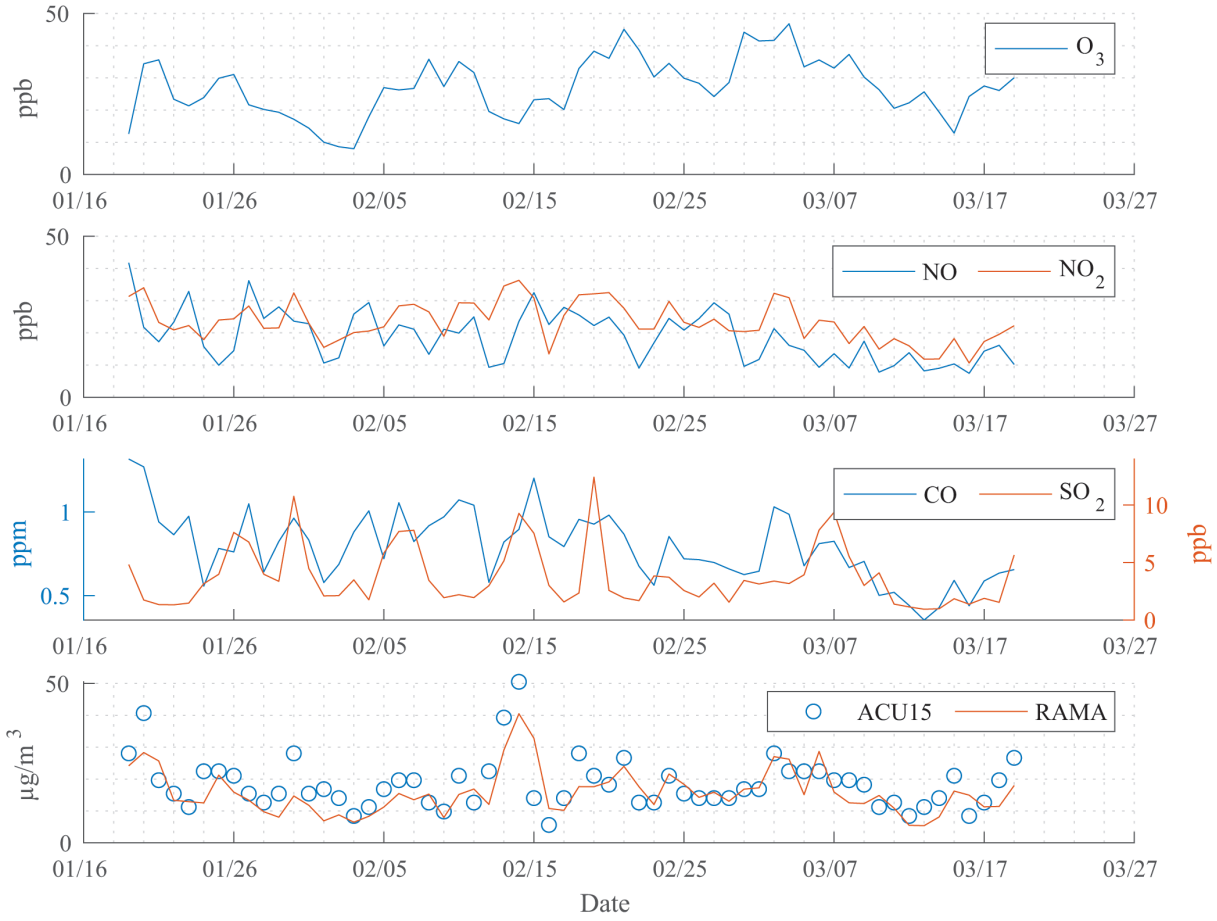

Figure 4. Daily average criteria pollutants during ACU15. Data source: RAMA.

of TC. If the total carbon from radiocarbon analysis (TCrc) has equal parts of pMC and fossil carbon (FC), then:

$$TC_{rc} = 0.5pMC + 0.5FC \quad (7)$$

(Rosa *et al.*, 2024) mention that the TC from thermal analysis (TCta) in $PM_{2.5}$ in the ACU15 campaign is formed by 25% primary organic carbon (POC), 50% secondary organic carbon (SOC), and 25% EC, so:

$$TC_{ta} = 0.25EC + 0.25POC + 0.50SOC \quad (8)$$

Equating equations 7 and 8 and assuming that EC and POC are exclusively fossil fuel combustion products, FC is formed by 0.5POC + 0.5EC, and the pMC corresponds to the SOC.

3.5 Elements

Al, Fe, and Si were grouped as soil elements related to the resuspension of road dust and earth crust material. Figure 5a shows a time series of soil element concentrations. Al and Si showed a correlation coefficient of 0.75, indicating the presence of aluminum silicates from soils (Figure 5b). The remaining elements (P, S, Cl, Cr, Mn, and Pb) were No soil elements (Figure 5c). Figure 5d shows P and S had a correlation coefficient of 0.91, meaning a solid association between sulfates and phosphates probably originated from gasoline combustion since both S and P are common additive agents in gasoline formulation (Hernández-López *et al.*, 2020).

Mercury was also present with an average concentration of 126 ± 3 pg m^{-3}; previous studies reported concentrations of 223 pg m^{-3} and 187 ± 3 pg m^{-3} in other sites of MCMA (Garza-Galindo *et al.*, 2019; Morton-Bermea, Hernández-Álvarez, *et al.*, 2021; Morton-Bermea, Schiavo, *et al.*, 2021; Schiavo *et al.*, 2022). The sources of Hg are linked to industrial activities, such as pigment or preservative material in electrical and medical equipment, luminaries, and lubricating oils. The maximum concentration of Hg measured was 310 pg m^{-3}, which is higher than the mercury vapor limit established by the World Health Organization; those values were measured in two samples.

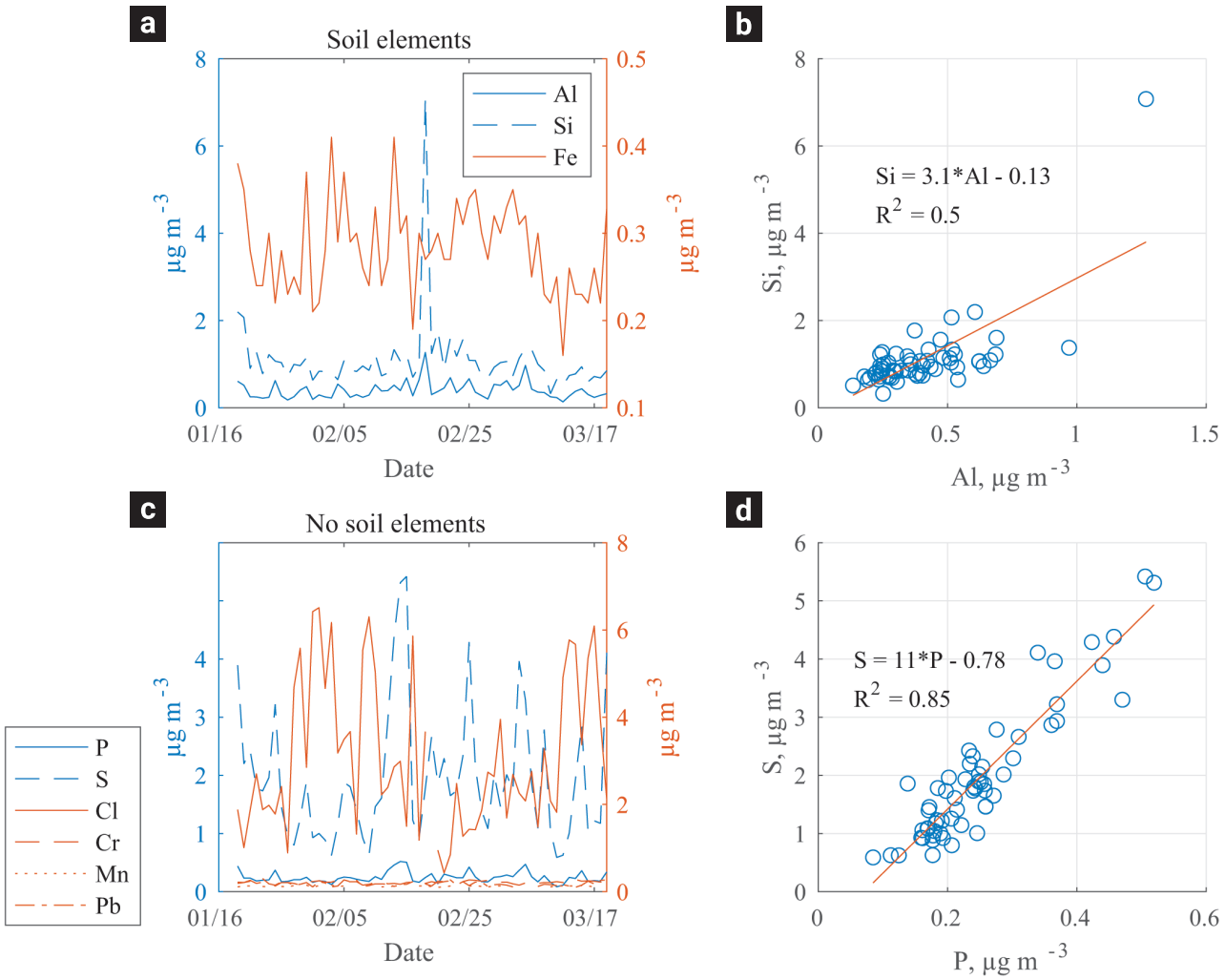

Figure 5. Elements on $PM_{2.5}$, a) time series of soil elements, b) scatter plot Al vs. Si, c) time series of No soil elements, and d) scatter plot P vs S.

3.6 Secondary inorganic aerosol

The IC and the ACSM measured NH_4^+, NO_3^-, and SO_4^{2-}, the most abundant components of SIA. In general, the IC measured lower concentrations than the ACSM. Table 2 shows the main results of both instruments.

According to (Salcedo *et al.*, 2018), ACSM measures non-refractory material with 1.0 µm aerodynamic diameter or less and may have an error ranging from -30 to +10%, which probably explains the differences between both analytical instruments' readings. However, the UIC and the ACSM measured similar concentrations of OC (Table 2).

Table 2. Comparison of ion chromatograph (IC) analysis, carbon analysis (UIC), and the aerosol chemical speciation monitor (ACSM). Concentrations are in µg m^{-3}.

	NO_3 IC	NO_3 ACSM	SO_4 IC	SO_4 ACSM	NH_4 IC	NH_4 ACSM	OC UIC	OC ACSM
n	50	52	50	53	53	54	59	54
min	0.23	0.35	0.31	0.71	0.30	0.33	4.48	2.68
max	3.38	5.83	4.46	11.13	1.98	5.44	13.19	16.58
average	1.00	2.53	1.80	4.20	1.03	1.89	8.06	8.36
std dev	0.66	1.36	1.11	2.63	0.48	1.08	1.85	3.22

The average total anion and cation concentrations measured by IC were 2.97 μg m^{-3} and 1.31 μg m^{-3}, respectively. SO_4^{2-}, NH_4^+, and NO_3^- correlated well with each other (Table 3), suggesting the presence of $(NH_4)_2SO_4$ and NH_4NO_3 produced by photochemical reactions due to emissions of gasoline and diesel exhaust compounds. The time series shows the equivalent concentrations of major (Figure 6a) and minor ions (Figure 6b) in equivalents.

The ratio K^+/Cl^- was 0.88 ± 0.61, meaning that the source was not just the biomass burning. The ratio NO_3^-/SO_4^{2-} was 0.76 ± 0.63, suggesting that vehicles with fossil fuel engines are the primary source of those ions. There is a good neutralization of ions in the particle, so the NR is 1.06. Figure 6c shows the time series of the sum of cations and anions in equivalent concentration. The linear regression slope was 0.96, with a determination coefficient of 0.85, so particulate matter had a scarcity of anions. There are other particle anions (i.e., CO_3^{2-}, PO_4^{3-}, OH^-) that were not measured and probably neutralized.

Table 3. Cross-correlation of oxidated species.

	NH_4^+	NO_3^-	SO_4^{2-}	SOC
NH_4^+	1.00	0.59	0.72	0.10
NO_3^-		1.00	0.38	-0.09
SO_4^{2-}			1.00	0.02
SOC				1.00

SOC had correlations close to zero with SIA components, so particles incorporated diverse oxidized compounds, semi and low-volatile organics, biological material, and other sources of organic species that probably did not directly originate from atmospheric secondary reactions. Table 4 shows the average ratios of chemical species concentration.

$PM_{2.5}$, OC, and EC concentrations are like two other extensive previous studies (Chow *et al.*, 2002; Vega *et al.*, 2004). However, the abundance of some ions has changed. Na^+, K^+, SO_4^{2-},

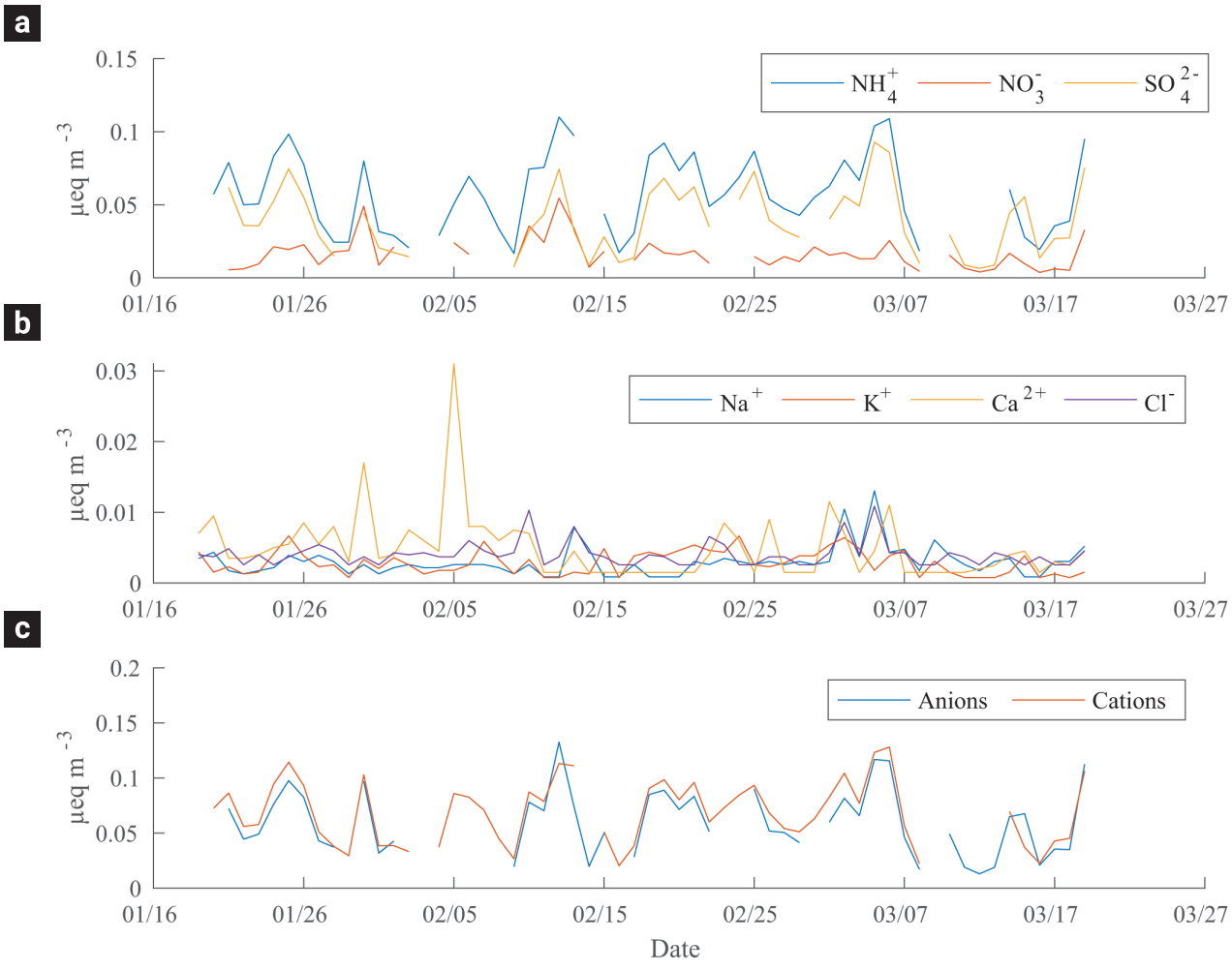

Figure 6. Time series of ion composition in $PM_{2.5}$, a) major ions, b) minor ion, and c) sum of equivalents.

and NH_4^+ are found in smaller amounts than previous studies, while Cl^- has increased. In the same way, Al, Mn, and Fe have increased. Crustal material and modifications in catalysts might cause those changes.

SO_4^{-2} and NH_4^+ showed a similar pattern between each other. Sulfate increased when the wind blew from the north. The average SOR was 0.35, indicating photo-oxidation of SO_2. The average NOR was 0.02. The average NO_3^-/SO_4^{2-} ratio was 1.12,

Table 4. Oxidation parameters on ACU15.

	SOR	NOR	NR	OC/EC	SOC/OC
N	50	50	42	44	44
min	0.08	0.00	0.43	1.40	0.00
max	0.63	0.05	1.71	9.56	0.85
average	0.35	0.02	1.06	3.74	0.54
std dev	0.15	0.01	0.19	1.79	0.20

Table 5. Species concentrations in $PM_{2.5}$ and atmospheric gases in ACU15, IMADA 1997 and 2002 in Mexico City.

ACU15/Pedregal AQ monitoring station			IMADA (1997)		VEGA 2000-2002		Millán-Vázquez *et al.*, 2023 (Merced)	
Specie	Average	Max	Average	Max	Average	Max	Average	Max
$PM_{2.5}$ (µg m^{-3})	20.52 ± 8.01	42.69	21.60	33.85	22.41	34.08	20.7	41.1
Carbonaceous aerosols (µg m^{-3})								
OC	8.06 ± 1.85	13.19	7.62	10.45	13.63	20.08		
EC	2.45 ± 1.69	7.28	2.89	4.38	3.81	6.27		
Total Carbon	10.51	20.47	10.50	13.97	17.16	26.13		
Ions (µg m^{-3})								
Na^+	0.07 ± 0.05	0.3	0.12	0.90	0.20	0.56	0.9	1.4
NH_4^+	1.03 ± 0.56	1.98	1.96	3.71	2.59	5.33	1.4	4.8
K^+	0.11 ± 0.07	0.27	0.16	0.26	0.14	0.79	0.2	2.6
Ca^{+2}	0.10 ± 0.09	0.62	0.17	0.40	0.14	0.92	0.5	3.1
Cl^-	0.14 ± 0.06	0.38	0.00	0.01	0.02	0.16	0.1	1.9
NO_3^-	1.00 ± 0.85	3.38	1.16	7.47	2.17	8.90	1.9	9.7
SO_4^{-2}	1.80 ± 1.23	4.46	4.53	8.81	5.29	11.87	4.3	13.4
Metals (µg m^{-3})								
Al	1.45 ± 0.69	3.56	0.17	0.45	0.05	0.67		
Si	0.70 ± 0.53	4.48	0.50	1.25	0.29	2.28		
P	0.28 ± 0.09	0.52	0.00	0.01	0.00	0.00		
S	1.47 ± 0.65	3.24	1.75	3.38	2.13	5.10		
Cr	0.22 ± 0.03	0.28	0.00	0.00	0.00	0.01		
Mn	0.12 ± 0.01	0.17	0.01	0.03	0.01	0.02		
Fe	0.28 ± 0.05	0.41	0.18	0.37	0.16	0.71		
Pb	0.18 ± 0.05	0.3	0.05	0.07	0.00	0.01		
Hg (pg m^{-3})	125.75 ± 3.10	310.26						
Criteria gases (ppb)								
O_3	27.07 ± 9.12	46.8						
NOx	42.18 ± 7.05	73.09						
NO_2	23.37 ± 12.18	36.32					46.1	97.1
SO_2	3.77 ± 6.17	12.42					7.8	35.2
CO	790 ± 210	1250						
Climate forcing gases (ppm)								
CO_2	420.52 ± 2.61	445.01						
CH_4	2.02 ± 0.74	2.34						
H_2O	0.96 ± 193.51	1.32						

which is common in areas where vehicular emissions dominate over coal or sulfur emissions, like the MCMA.

Table 4 shows the NOR, SOR, NR, OC/EC, and SOC statistics. SOR average is 0.35 and NOR 0.02. Both values are like those reported in 2021 (Millán-Vázquez *et al.*, 2023) for La Merced, a measuring site in Mexico City downtown. Both sites have identical oxidation rates, although Merced has a higher concentration of sulfates. The study of 2002 (Vega *et al.*, 2004) reported a pMC of 60% for an industrial zone and a pMC of 76% for a residential zone in Mexico City. The pMC estimated in ACU15 indicates a significant intensification (10% to 16%) in the contribution of fossil sources relative to previous measurements. That result is consistent with the substantial increase in the vehicular fleet in recent years and probably the loss of green areas in MCMA (Lima *et al.*, 2023).

We found a particle chemical composition like IMADA and 2000 studies. In 2021, (Mill.n-V.zquez *et al.*, 2023) found similar results in Merced in downtown Mexico City (Millán-Vázquez *et al.*, 2023). For the previous studies, there have been no significant changes in carbon content, inorganic ions composition, or elements content in $PM_{2.5}$, probably meaning that the efforts in reducing and controlling the emissions sources of particles into the atmosphere have shown poor results (Table 5). For the study of 2021, the concentration of pollutants in ACU15 is lower than in Merced. Poor transport of contaminants from the south and minor local activities are probably the leading causes of low concentrations in ACU15.

Figure 7 shows the comparison of $PM_{2.5}$ composition with two previous studies. The concentration of $PM_{2.5}$, OC, EC, water-soluble inorganic ions, and elements is slightly lower in ACU15. The poor or null transport of material from other sites in the south, the local activities, and the diversity of particle sources probably explain the different particle compositions.

4. Discussion

(Zhao *et al.*, 2022) reported an average NOR of 0.11 and SOR of 0.76 for Wuhan in 2015. (Millán-Vázquez *et al.*, 2023) reported SOR of 0.21 and NOR 0.015 for Mexico City in 2021. In ACU15, the average SOR was 0.35 and NOR 0.01. Mexico City's NOR is ten times lower than Wuhan's, meaning that the amount of atmospheric NO_2 has a slow conversion rate.

Based on wind speed and HYSPLIT, distant sources probably had a low influence on the local air quality. Elements from crustal origin, soil dust, asphalt, and unpaved roads contributed to nearly 22% of $PM_{2.5}$ mass, and the abundance of elements was 3.8%. Hg had a low concentration and is probably related to industrial activities. The water-soluble inorganic ions represent 11% of $PM_{2.5}$ mass. Unknown species represent 4% of $PM_{2.5}$ mass.

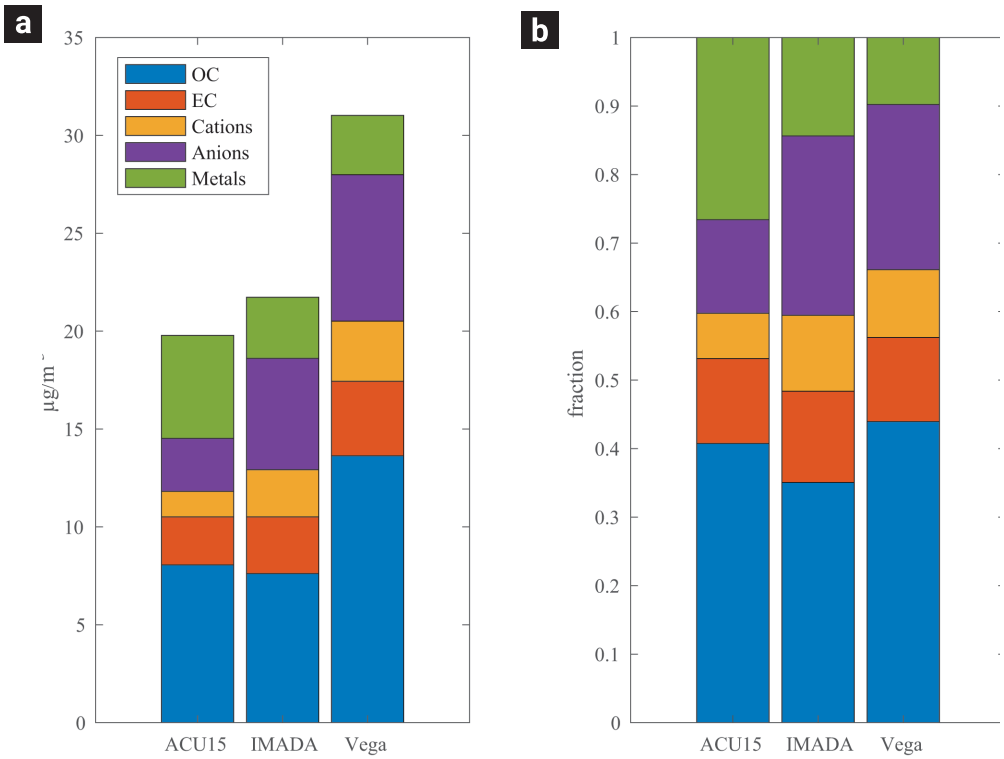

Figure 7. a) Mass composition and b) fraction of mass composition of $PM_{2.5}$ in Mexico City during three measuring campaigns (IMADA 1997, Vega *et al.*, 2002, and ACU15 2015).

The average EC measured during the campaign was 2.4 ± 1.7 μg m^{-3}. Also, OC is the most abundant species of $PM_{2.5}$, with 39% in mass, and SOC corresponds to half of OC. Therefore, biological contribution, organic condensation, and secondary atmospheric reactions probably form half of the organic carbonaceous aerosols.

Radiocarbon analysis indicated that 50% of TC originates from burning fossil fuels, and the rest contain biogenic and other contemporary sources. The measurement site is in a typical urban zone with regular vehicular traffic, and half of the fossil carbon corresponds to EC and the rest to POC. The modern carbon corresponded to SOC.

The OC/EC ratio of 3.29 is in the range of 2.5 – 5.0 that are considered for a carbonaceous fraction from vehicle exhaust and include large amounts of secondary organics (G. Li *et al.*, 2011; K. Li *et al.*, 2018; L. Li *et al.*, 2019; S. Li *et al.*, 2022; X. Li *et al.*, 2018; Pósfai *et al.*, 2003; F. Zhang *et al.*, 2013; Y. Zhang *et al.*, 2018). Although the monitoring site is 300 m away from the metro and bus stations, the composition of $PM_{2.5}$ does not reflect a unique fossil fuel influence.

5. Conclusions

Clean air often blew from the south, so the $PM_{2.5}$ average concentration was 20.52 μg m^{-3}, so our results describe the local $PM_{2.5}$. The radiocarbon data shows an equal contribution of contemporary and fossil sources to TC. $PM_{2.5}$ had high concentrations of OC, high crust soil composition, and low SIA. The SO_2 reacts to SO_4^{2-}, like other cities (i.e., Wuhan), but the NO_2 was not photo-oxidated to NO_3^-. Sulfur and phosphorus had a high correlation, indicating fossil fuel combustion. We have not found conclusive evidence indicating an improvement in air quality in terms of $PM_{2.5}$ composition since 2000. The composition of particulate matter has changed slightly compared to the 1997, 2000, and 2021 studies, but this does not necessarily imply lower toxicity of particulate matter. The NR indicated a close-to-neutral atmosphere.

Most of the elements present in the particles are from crustal material and soils, and even though heavy metals were detected, their concentrations were low enough to be considered dangerous pollutants.

6. Acknowledgments

The authors thank Mariana Avila, María Rodríguez, and Sergio Martínez for technical assistance. We also want to thank Arcadio Huerta for supporting radiocarbon-AMS analyses. We also thank the ECAIM Project for its funding support.

7. Referencias

Abanto, R. L., Castro, T., Peralta, O., Suarez, L. G. R., Salcedo, D., Carabali, G., *et al.* (2020). Mediciones continuas de carbono negro, monóxido de carbono y dióxido de carbono, durante la temporada seca caliente 2016, en un sitio periurbano de Querétaro, México. *Ciencia & Desarrollo*, 19(26), 68–76. doi: **https://doi.org/10.33326/26176033.2020.26.934**

Alvarez-Ospina, H., Peralta, O., Castro, T., & Saavedra, M. I. (2016). Optimum quantification temperature for total, organic, and elemental carbon using thermal-coulombimetric analysis. *Atmospheric Environment*, 145(2016), 74–80. doi: **https://doi.org/10.1016/j.atmosenv.2016.08.080**

Bozkurt, H., D'Souza, D. H., & Davidson, P. M. (2014). Determination of thermal inactivation kinetics of hepatitis A virus in blue mussel (Mytilus edulis) homogenate. *Applied and Environmental Microbiology*, 80(10), 3191–7. doi: **https://doi.org/10.1128/aem.00428-14**

Chow, J. C., Watson, J. G., Edgerton, S. A., & Vega, E. (2002). Chemical composition of PM2.5 and PM10 in Mexico City during winter 1997. *Science of The Total Environment*, 287(3), 177–201. doi: **https://doi.org/10.1016/s0048-9697(01)00982-2**

Chu, W., Li, L., Li, H., Zhang, Y., Chen, Y., Zhi, G., *et al.* (2023). Atmospheric Oxidation Capacity and Its Impact on the Secondary Inorganic Components of PM2.5 in Recent Years in Beijing: Enlightenment for PM2.5 Pollution Control in the Future. *Atmosphere*, 14(8), 1252. doi: **https://doi.org/10.3390/atmos14081252**

Dat, N.-Q., Ly, B.-T., Nghiem, T.-D., Nguyen, T.-T. H., Sekiguchi, K., Huyen, T.-T., *et al.* (2024). Influence of Secondary Inorganic Aerosol on the Concentrations of PM2.5 and PM0.1 during Air Pollution Episodes in Hanoi, Vietnam. *Aerosol and Air Quality Research*, 24(4), 220446. doi: **https://doi.org/10.4209/aaqr.220446**

Davidson, C. I., Phalen, R. F., & Solomon, P. A. (2007). Airborne Particulate Matter and Human Health: A Review. *Aerosol Science and Technology*, 39(8), 737–749. doi: **https://doi.org/10.1080/02786820500191348**

Echeverría, R. S., Jiménez, A. L. A., Barrera, M. del C. T., Alvarez, P. S., Hernandez, E. G., Vega, E., *et al.* (2023). Nitrogen and sulfur compounds in ambient air and in wet atmospheric deposition at Mexico city metropolitan area. *Atmospheric Environment*, 292, 119411. doi: **https://doi.org/10.1016/j.atmosenv.2022.119411**

Evans, J. S., Rojas-Bracho, L., Hammitt, J. K., & Dockery, D. W. (2021). Mortality Benefits and Control Costs of Improving Air Quality in Mexico City: The Case of Heavy Duty Diesel Vehicles. *Risk Analysis*, 41(4), 661–677. doi: **https://doi.org/10.1111/risa.13655**

Garza-Galindo, R., Morton-Bermea, O., Hernández-Álvarez, E., Ordoñez-Godínez, S. L., Amador-Muñoz, O., Beramendi-Orosco, L. E., *et al.* (2019). Spatial and temporal distribution of metals in PM2.5 during 2013: assessment of wind patterns to the impacts of geogenic and anthropogenic sources. *Environmental Monitoring and Assessment*, 191(3), 165. doi: **https://doi.org/10.1007/s10661-019-7251-4**

Garzón, J. P., Huertas, J. I., Magaña, M., Huertas, M. E., Cárdenas, B., Watanabe, T., *et al.* (2015). Volatile organic compounds in the atmo-

sphere of Mexico City. *Atmospheric Environment*, 119, 415–429. doi: **https://doi.org/10.1016/j.atmosenv.2015.08.014**

Hernández-López, A. E., Campo, J. M. M. del, Mugica-Álvarez, V., Hernández-Valle, B. L., Mejía-Ponce, L. V., Pineda-Santamaría, J. C., *et al.* (2020). A study of pm2.5 elemental composition in southwest mexico city and development of receptor models with positive matrix factorization. *Revista Internacional de Contaminación Ambiental*. 37, 54066. doi: **https://doi.org/10.20937/rica.54066**

Instituto Nacional de Ecología y Cambio Climático. (2016). *Evolución de la calidad del aire de la ZMVM y episodios de ozono durante la temporada seca-caliente 2016*. Instituto Nacional de Ecología y Cambio Climático

Instituto Nacional de Estadística y Geografía (2017). *Anuario estadístico y geográfico de la Ciudad de México 2017*. Instituto Nacional de Estadística y Geografía, México.

Li, G., Bei, N., Tie, X., & Molina, L. (2011). Aerosol effects on the photochemistry in Mexico City during MCMA-2006/MILAGRO campaign. *Atmospheric Chemistry And Physics*, 11, 5169-5182. doi: **https://doi.org/10.5194/acp-11-5169-2011**

Li, K., Jacob, D. J., Liao, H., Shen, L., Zhang, Q., & Bates, K. H. (2018). Anthropogenic drivers of 2013–2017 trends in summer surface ozone in China. *Proceedings of the National Academy of Sciences*, 116(2), 201812168. doi: **https://doi.org/10.1073/pnas.1812168116**

Li, L., Wang, Q., Zhang, X., She, Y., Zhou, J., Chen, Y., *et al.* (2019). Characteristics of single atmospheric particles in a heavily polluted urban area of China: size distributions and mixing states. *Environmental Science and Pollution Research*, 1–13. doi: **https://doi.org/10.1007/s11356-019-04579-3**

Li, S., Chen, C., Yang, G., Fang, J., Sun, Y., Tang, L., *et al.* (2022). Sources and processes of organic aerosol in non-refractory PM1 and PM2.5 during foggy and haze episodes in an urban environment of the Yangtze River Delta, China. *Environmental Research*, 113557. doi: **https://doi.org/10.1016/j.envres.2022.113557**

Li, X., Li, S., Xiong, Q., Yang, X., Qi, M., Zhao, W., & Wang, X. (2018). Characteristics of PM2.5 Chemical Compositions and Their Effect on Atmospheric Visibility in Urban Beijing, China during the Heating Season. International *Journal of Environmental Research and Public Health*, 15(9), 1924. doi: **https://doi.org/10.3390/ijerph15091924**

Lima, G. N. de, Fonseca-Salazar, Ma. A., & Campo, J. (2023). Urban growth and loss of green spaces in the metropolitan areas of São Paulo and Mexico City: effects of land-cover changes on climate and water flow regulation. *Urban Ecosystems*, 26(6), 1739–1752. doi: **https://doi.org/10.1007/s11252-023-01394-0**

Mamkhezri, J., Bohara, A. K., & Camargo, A. I. (2020). Air pollution and daily mortality in the Mexico City Metropolitan Area. *Atmósfera*. 33(3). doi: **https://doi.org/10.20937/atm.52557**

Millán-Vázquez, F., Sosa-Echevería, R., Alarcón-Jiménez, A. L., Figueroa-Lara, J. de J., Torres-Rodríguez, M., Valle-Hernández, B. L., & Mugica-Álvarez, V. (2023). Temporal Variation and Potential Sources of Water-Soluble Inorganic Ions in PM2.5 in Two Sites of Mexico City. *Atmosphere*, 14(10), 1585. doi: **https://doi.org/10.3390/atmos14101585**

Morton-Bermea, O., Hernández-Álvarez, E., Ordoñez-Godínez, S. L., & Montes-Ávila, I. (2021). Mercury, Platinum, Antimony and Other Trace Elements in the Atmospheric Environment of the Urban Area of Mexico City: Use of Ficus benjamina as Biomonitor. *Bulletin of Environmental Contamination and Toxicology,* 106(4), 665–669. doi: **https://doi.org/10.1007/s00128-020-03080-9**

Morton-Bermea, O., Schiavo, B., Salgado-Martínez, E., Almorín-Ávila, M. A., & Hernández-Álvarez, E. (2021). Gaseous Elemental Mercury (GEM) in the Mexico City Metropolitan Area. *Bulletin of Environmental Contamination and Toxicology,* 107(3), 514–518. doi: **https://doi.org/10.1007/s00128-021-03293-6**

Pósfai, M., Simonics, R., Li, J., Hobbs, P. V., & Buseck, P. R. (2003). Individual aerosol particles from biomass burning in southern Africa: 1. Compositions and size distributions of carbonaceous particles. *Journal of Geophysical Research: Atmospheres* (1984–2012), 108(D13). doi: **https://doi.org/10.1029/2002jd002291**

Prieto, C., Alvarez-Ospina, H., Salcedo, D., Castro, T., & Peralta, O. (2023). Mass Absorption Efficiency of PM1 in Mexico City during ACU15. *Atmosphere*, 14(1), 100. doi: **https://doi.org/10.3390/atmos14010100**

Rosa, N. S. la, Prieto, C., Pavia, R., Peralta, O., Alvarez-Ospina, H., Saavedra, I., *et al.* (2024). Carbonaceous particles and PM2.5 optical properties in Mexico City during the ACU15 campaign. *Atmósfera*, 38, 369–380. doi: **https://doi.org/10.20937/atm.53270**

Salcedo, D., Alvarez-Ospina, H., Peralta, O., & Castro, T. (2018). PM1 Chemical Characterization during the ACU15 Campaign, South of Mexico City. *Atmosphere*, 9(6), 232. doi: **https://doi.org/10.3390/atmos9060232**

Schiavo, B., Morton-Bermea, O., Salgado-Martínez, E., García-Martínez, R., & Hernández-Álvarez, E. (2022). Health risk assessment of gaseous elemental mercury (GEM) in Mexico City. *Environmental Monitoring and Assessment*, 194(7), 456. doi: **https://doi.org/10.1007/s10661-022-10107-7**

Secretaría del Medio Ambiente de la Ciudad de México. (2021). *Inventario de Emisiones de la Zona Metropolitana del Valle de México 2018.* Secretaría del Medio Ambiente de la Ciudad de México

Sharma, S. K., Mandal, T. K., Sharma, A., Saraswati, & Jain, S. (2018). Seasonal and annual trends of carbonaceous species of PM10 over a megacity Delhi, India during 2010–2017. *Journal of Atmospheric Chemistry*, 75(3), 305–318. doi: **https://doi.org/10.1007/s10874-018-9379-y**

Squizzato, S., Masiol, M., Brunelli, A., Pistollato, S., Tarabotti, E., Rampazzo, G., & Pavoni, B. (2013). Factors determining the formation of secondary inorganic aerosol: a case study in the Po Valley (Italy). *Atmospheric Chemistry and Physics*, 13(4), 1927–1939. doi: **https://doi.org/10.5194/acp-13-1927-2013**

Turpin, B. J., & Huntzicker, J. J. (1995). Identification of secondary organic aerosol episodes and quantitation of primary and secondary

organic aerosol concentrations during SCAQS. *Atmospheric Environment*, 29(23), 3527–3544. doi: **https://doi.org/10.1016/1352-2310(94)00276-q**

Vega, E., Reyes, E., Ruiz, H., García, J., Sánchez, G., Martínez-Villa, G., *et al.* (2004). Analysis of PM2.5and PM10 in the Atmosphere of Mexico City during 2000-2002. *Journal of the Air & Waste Management Association*, 54(7), 786–798. doi: **https://doi.org/10.1080/10473289.2004.10470952**

Warneke, C., Gouw, J. A. de, Edwards, P. M., Holloway, J. S., Gilman, J. B., Kuster, W. C., *et al.* (2013). Photochemical aging of volatile organic compounds in the Los Angeles basin: Weekday-weekend effect. *Journal of Geophysical Research*.118(10), 5018-5028. doi: **https://doi.org/10.1002/jgrd.50423**

Zavala, M., Brune, W. H., Velasco, E., Retama, A., Cruz-Alavez, L. A., & Molina, L. T. (2020). Changes in ozone production and VOC reactivity in the atmosphere of the Mexico City Metropolitan Area. *Atmospheric Environment*, 238, 117747. doi: **https://doi.org/10.1016/j.atmosenv.2020.117747**

Zhang, F., Xu, L., Chen, J., Chen, X., Niu, Z., Lei, T., *et al.* (2013). Chemical characteristics of PM2.5 during haze episodes in the urban of Fuzhou, China. *Particuology*, 11(3), 264–272. doi: **https://doi.org/10.1016/j.partic.2012.07.001**

Zhang, Y., Zhang, Q., Cheng, Y., Su, H., Li, H., Li, M., *et al.* (2018). Amplification of light absorption of black carbon associated with air pollution. *Atmospheric Chemistry and Physics*, 18(13), 9879–9896. doi: **https://doi.org/10.5194/acp-18-9879-2018**

Zhao, J., Ma, C., He, C., Zhang, Z., Jiang, T., Tang, R., & Chen, Q. (2022). Variations in Sulfur and Nitrogen Oxidation Rates in Summer Aerosols from 2014 to 2020 in Wuhan, China. *Atmosphere*, 13(8), 1199. doi: **https://doi.org/10.3390/atmos13081199**